Effect of the growth conditions on the spatial features of Re nanowires produced by directional solidification

ARTICLE *in* NANO LETTERS · MAY 2006

Impact Factor: 13.59 · DOI: 10.1021/nl0514238 · Source: PubMed

3 AUTHORS, INCLUDING:

Srdjan Milenkovic
Madrid Institute for Advanced Studies
60 PUBLICATIONS **588** CITATIONS
SEE PROFILE

Achim Walter Hassel
Johannes Kepler University Linz
182 PUBLICATIONS **2,119** CITATIONS
SEE PROFILE

NANO LETTERS

2006
Vol. 6, No. 4
794−799

Effect of the Growth Conditions on the Spatial Features of Re Nanowires Produced by Directional Solidification

Srdjan Milenkovic, Achim Walter Hassel,* and André Schneider

Max-Planck-Institut für Eisenforschung GmbH, Max-Planck-Strasse 1, D-40237 Düsseldorf, Germany

Received July 22, 2005; Revised Manuscript Received December 4, 2005

ABSTRACT

The effects of the solidification parameters, such as growth rate and temperature gradient, on the distance and diameter of Re nanowires have been examined. Both the spacing and diameter increase with decreasing growth rate and temperature gradient, respectively. The ratio of fiber spacing to diameter is 9.1. In addition, it was demonstrated that the temperature gradient influences interface undercooling in the same way as the growth rate and may be used as an additional parameter to control fiber spacing and diameter.

Introduction. One-dimensional nanostructures have attracted significant research interest due to their mechanical, electrical, magnetic, and optical properties. Besides, they provide models to study the relationship between electrical transport and optical and other properties with dimensionality and size confinement. Recently, we have developed a novel method for assembling nanowire and nanopore arrays via directional solidification and selective etching of eutectic alloys.[1,2] One of the crucial factors in the synthesis of nanowires is the microstructural control governed by the kinetics of the solidification process.

The directional solidification of eutectic alloys under controlled growth conditions generally yields lamellar or fibrous structures, aligned parallel to the direction of heat extraction, i.e., the growth direction. Two important parameters of eutectic structure, which are influenced by the imposed process parameters, are the phase diameter and the eutectic spacing. The classical theory of eutectic growth was proposed by Jackson and Hunt[3] in mid 1960s. To obtain an analytical solution for the diffusion problem at the solid/liquid interface, they assumed a planar interface and equal undercooling of both solid phases growing in a coupled mode from a melt of eutectic composition. Jackson and Hunt[3] postulated a relationship between total interface undercooling, the solute concentration field, and the interface curvature. Since their analysis was derived from the Zenner[4] and Tiller[5] treatment of eutectic growth, it was necessary to introduce an arbitrary extremum condition because the problem would have been intrinsically indeterminate without it. Considering the minimal undercooling as the "extremum condition", i.e., that eutectic growth occurs near or at minimal undercooling, Jackson and Hunt obtained a series of relations between fiber (or lamellae) spacing, solidification velocity and average undercooling. The average undercooling for fiber eutectic structures, being a sum of the constitutional and capillary undercooling could be expressed as

$$\Delta T = K_1 \lambda V + \frac{K_2}{\lambda} \tag{1}$$

where λ is the distance between fibers, ΔT is the undercooling of the solidification front, V is the solidification velocity, and K_1 and K_2 are summarized material parameters (see ref 3). The minimum undercooling criterion leads to

$$\lambda^2 V = \frac{K_2}{K_1} \tag{2a}$$

$$\frac{\Delta T}{\sqrt{V}} = 2\sqrt{K_1 K_2} \tag{2b}$$

$$\Delta T \lambda = 2K_2 \tag{2c}$$

which is well accepted and has been experimentally verified many times.[6] The formation of eutectic structures was theoretically reviewed in recent years and to a certain extent also verified or confirmed experimentally. Many investigations for eutectic spacing have been performed in the lamellar eutectics, whereas there is little concern for the relationship between the fiber spacing and the controlling parameters in fibrous or rodlike eutectic alloy. Moreover, the relationship between the fiber diameter and the growth parameters has not been reported yet. Considering it of crucial importance for our investigations, to know the range of nanowires that can be produced, this aspect is analyzed as well. This work presents an experimental investigation on the pseudobinary NiAl−Re eutectic system, with the main objective to

* Corresponding author: E-mail: hassel@elchem.de.

10.1021/nl0514238 CCC: $33.50
Published on Web 04/12/2006

investigate the effect of processing parameters on spatial features, namely, spacing and diameter, of the Re nanowires produced by directional solidification.

Experiments. Microstructure of directionally solidified eutectics is essentially controlled by alloy composition, growth rate, and temperature gradient. In this study, rhenium concentration was carefully controlled to conform to the eutectic composition. According to the NiAl−Re phase diagram proposed by Rablbauer et al.,[7] eutectic reaction occurs at NiAl−1.5 atom % Re at 1674 °C. Prealloys were prepared from nickel (99.97 wt %), electrolytic aluminum (99.9999 wt %), and rhenium pellets (99.9 wt %) by induction melting under inert atmosphere and drop casting into a cylindrical copper mold. Subsequently, the as cast ingots were placed in alumina crucibles and directionally solidified in a Bridgman type crystal growing facility. It consists of the crucible support, cooling ring, and heating element (tungsten net). The alumina crucible with the as-cast ingot was positioned in the furnace and heated to ∼1700 °C. After complete melting of the material in the crucible, the upper part with the heating element is slowly and uniformly shifted upward, providing thus unidirectional heat extraction. This operation was controlled by a servomotor that enabled a speed range from 1 to 55 μm s^{-1}. The temperature of the Bridgman-type furnace was controlled by a Pt/Pt−18% Rh thermocouple placed between the heating element and the alumina tube. The temperature could be controlled to about ±0.1 K during the run. For the temperature gradient measurement, type C W/Re thermocouples were placed into protective capillary alumina tubes (0.8 mm i.d., 1.2 mm o.d.) and positioned 20 mm apart and parallel to the heat flow direction in the crucible. The temperature gradients are calculated straightforward, dividing the temperature difference between two thermocouples by the separation distance between them. The experiments were conducted with a constant temperature gradient and different growth rates, including the lowest and the highest rates available (1−55 μm s^{-1}), as well as with a constant growth rate and different temperature gradients (40−60 K cm^{-1}).

Directionally solidified ingots were removed from the crucibles, cut in transverse sections, and prepared by grinding and mechanical and chemical polishing for further metallographic analysis. The analysis included morphology examination as well as fiber spacing and diameter measurements using optical and scanning electron microscopy. To determine fiber spacing, fault-free regions of cross-sectional samples were selected and the line-intercept method was utilized. The variations of fiber spacing λ with respect to G and V were determined by using linear regression analysis. In addition, to get a better characterization of the microstructure, the influence of the processing parameters on the fiber diameter was evaluated. Therefore, 10 SEM pictures distributed arbitrarily over a section to avoid measuring localized effects were analyzed on each cross section. The values for the fiber distance and diameter have been averaged for each image, and the values are averaged for the 10 images that belong to one cross section. A JEM-2000CX scanning electron microscope was used for metallographic observations.

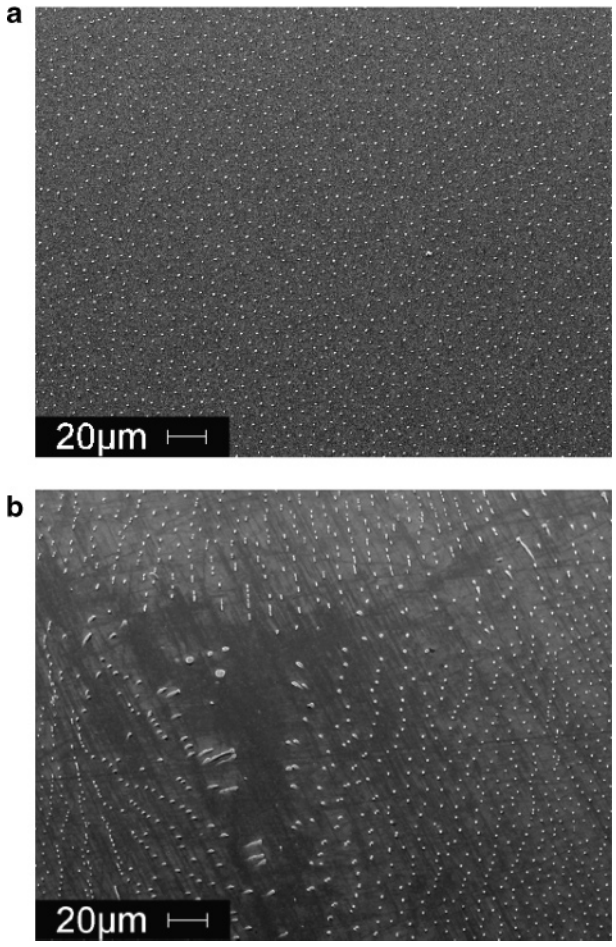

Figure 1. Typical microstructure of the directionally solidified NiAl−Re eutectic: (a) planar; (b) cellular.

Results and Discussion. (A) Microstructure. Typical microstructure of the directionally solidified NiAl−Re eutectics grown in this study is shown in Figure 1. For a range of solidification conditions (growth rates from 1.4 to 55.5 μm s^{-1} at gradients of 40 and 60 K cm^{-1}), a fully eutectic structure devoid of any dendritic regions was observed throughout the cross sections of the specimens. In the micrographs throughout the paper, the NiAl phase is the matrix and the Re phase the continuous fibers. Although the microstructure was constant along the rod, it varied with the solidification conditions. A planar eutectic microstructure was observed at low and intermediate growth rates (1.4 and 8.3 μm s^{-1}), where the boundaries of the eutectic colonies were easily discernible due to a change in the orientation of the fibers at colony boundaries (Figure 1a). However, at high growth rates (55.5 μm s^{-1}) cellular microstructures were observed with the Re fibers emanating radially from the cell interior to the cell boundaries, as shown in Figure 1b. The formation of the eutectic colony structure has been associated to the combined effects of the impurities rejected from the solidifying eutectic, the growth rate, and the imposed thermal gradient at the solid/liquid interface, which produce a zone of constitutionally undercooled liquid ahead of the growing interface. Under these conditions of growth, the planar solid/liquid interface becomes unstable and transforms into cellular interface. The growth characteristics of the colony structure

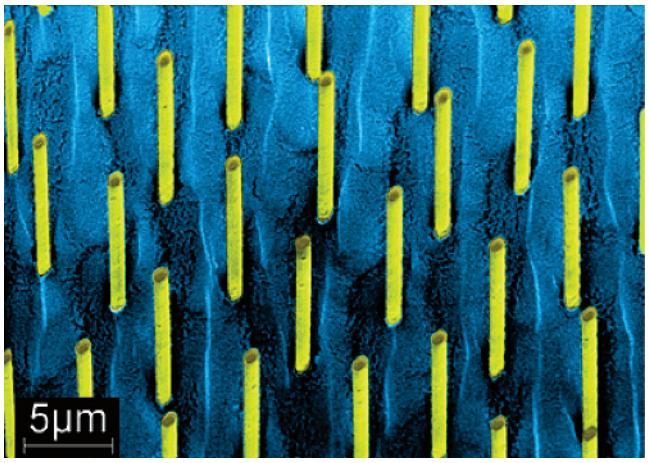

Figure 2. Re nanowires after selective etching of the NiAl matrix.

have been investigated by several researchers,[8−10] and it has been shown that the colonies are formed by the motion of a cellular solid/liquid interface during growth. Further, it was observed that fibers do not grow parallel to each other within the cells but diverge toward colony boundaries and tend to increase in thickness as they approach it. The direction in which the fibers grow in the cells gives a direct indication of the shape of the growing cellular interface. The formation of cell structure indicated that the applied growth conditions were below critical ones for achieving the planar solid/liquid interface.

To obtain nanowires from these initial microstructures, an appropriate and selective etching of the NiAl matrix is required. This procedure gives a structure in which rhenium nanowires stick parallel to each other in a corroded matrix, as shown in Figure 2. Depending on the etching time, the length of the nanowires can be easily controlled. Advantages

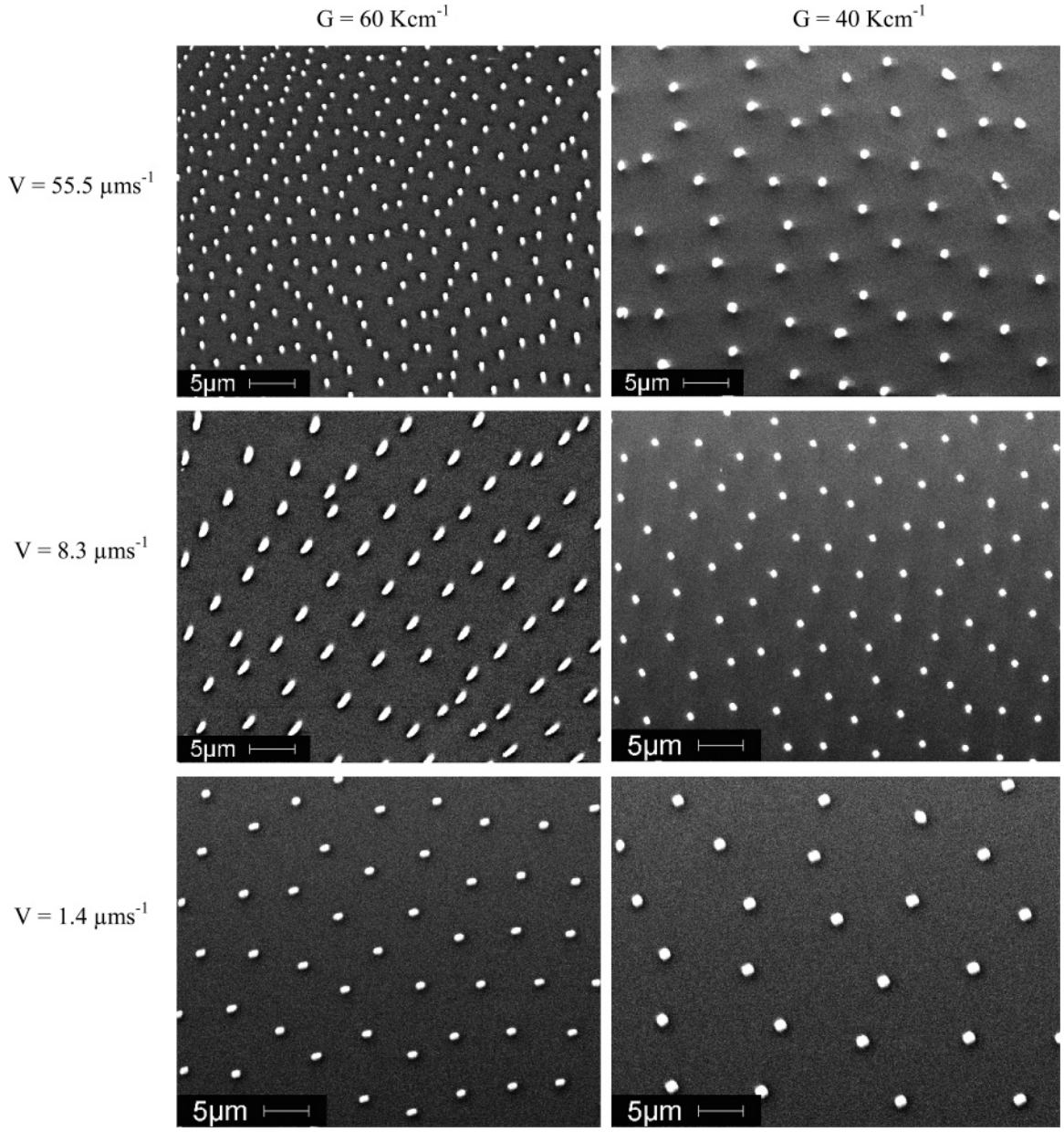

Figure 3. Microstructures obtained at different growth conditions.

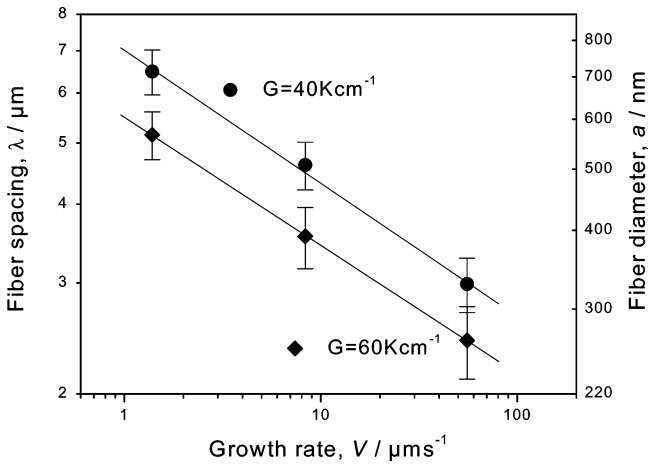

Figure 4. Influence of the growth rate on the fiber spacing, λ, and the fiber diameter, a.

of the nanowires produced are that they are self-organized, have high aspect ratio, and are single crystalline. In addition the selective etching of the matrix provides closer insight into the fiber morphology and enables examinations of microstructures in three dimensions In fact, the large depth of focus of the scanning electron microscope makes it possible to view both the longitudinal and the transverse sections simultaneously, as depicted in Figure 2.

(B) Effect of the Growth Rate. A significant aspect of eutectic growth under directional solidification conditions is the relationship between the growth rate V and the fiber spacing λ. As aforementioned the relationship between the inverse square root of the growth rate, V, and fiber spacing, λ, is linear, and generally, experimental results obey the above relationship. The fiber spacing, defined as the average distance on a transverse section between the centers of adjacent Re fibers, and the fiber size, defined as the average diameter of the cross sections, were measured over a range of growth rates, V, from 1.4 to 55.5 μm s^{-1} at temperature gradients of 40 and 60 K cm^{-1}, respectively. Figure 3 shows examples of the typical microstructures obtained for each growth condition. In Figure 4 fiber spacing, λ, is fitted by linear regression against the growth rate, V. It can be observed that a decrease in the growth rate from 55.5 to 1.4 μm s^{-1} leads to an increase in the fiber spacing from 2.4 to 5.5 μm, which means that the relationship $\lambda^2 V =$ constant holds in this system as well. When the growth rate increases, the effect of the lateral diffusion flux along the solid/liquid interface diminishes and boundary layer thickness increases. These changes in the growth conditions at solid/liquid interface lead to a decrease in fiber spacing. Evaluating Figure 4, a log−log plot of the growth rate versus fiber spacing, the constant K is calculated to be 2.19×10^{-16} m^3 s^{-1}. This constant holds for the investigated range of growth rates. However, further investigations over a wider range of growth rates would be desirable. For a diffusion controlled eutectic growth condition, the constant K is unique for each eutectic system and its value determines the influence of the growth rate on the fiber spacing.

Considering constant volume fraction of the phases for the given conditions, a change in fiber spacing affects fiber size accordingly. Nevertheless, the relation between the growth conditions and fiber size has attracted little interest in the research community. Since this microstructural feature is more important for our studies, we modified the existing relationship between fiber spacing and growth rate in order to obtain the straightforward relation between the growth rate and fiber diameter. The fiber diameter, a, is related to the fiber spacing, λ, and the volume fraction of the fibers, V_f, by

$$a^2 = gV_f\lambda^2 \tag{4}$$

where g is the geometrical factor dependent on the fiber arrangement. Substituting eq 4 in eq 2a, the following relationship between fiber size and growth rate is obtained

$$a^2V = K_3 \tag{5}$$

where K_3 is another constant. From eqs 4 and 5 it is seen that both fiber size and spacing are expected to vary inversely with the square root of growth rate. Using the same data from Figure 4 the following relations between V and λ and V and a were computed

$$\lambda^2V = 2.19 \times 10^{-16}\ \mathrm{m^3\ s^{-1}}$$
$$a^2V = 2.65 \times 10^{-18}\ \mathrm{m^3\ s^{-1}} \tag{6}$$

From eq 6, the ratio of fiber spacing to diameter, λ/a, is found to be 9.1, which gives a straightforward relationship between fiber spacing and diameter.

(C) Effect of the Temperature Gradient. The influence of the temperature gradient G on V has not been considered in theoretical studies. However, its influence cannot be ignored for regular and irregular eutectic systems, as several studies confirmed the influence of temperature gradient on the lamellar spacing.[11−14] Thus, one may expect similar influence of the temperature gradient on the fiber spacing.

To investigate the influence of the thermal gradient on the fiber spacing, first the experimental relationship between these two variables was established, as depicted in Figure 5. It can be observed that for a given constant growth rate, fiber spacing decreases with an increase in the temperature gradient. Considering that only two values of temperature gradients are used, the present analysis does not permit to correctly quantify the observed effect. Nevertheless, the qualitative nature of the effect may be derived. Since only two different temperature gradients were achievable, its effect was tested at three different growth rates. As may be observed from Figure 5 in all three cases, the same general tendency toward the relationship of type $\lambda \sim G^n$ was observed. This relationship can be written in a general form

$$\lambda = K_4G^{-0.5} \tag{7}$$

If we now substitute eq 7 in eq 1 and apply the condition of

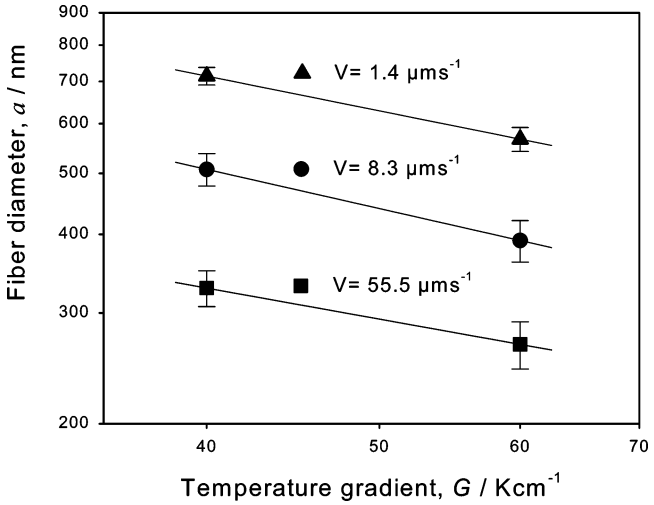

Figure 5. Influence of the temperature gradient on the fiber spacing, λ, and the fiber diameter, a.

growth at minimum undercooling ($(\partial\Delta T/\partial G)_V = 0$), eq 1 yields

$$V = \frac{K_2}{K_1 K_4^2} G \tag{8}$$

Using eq 8 in eq 1 gives

$$\Delta T = K_5 \lambda G + \frac{K_2}{\lambda} \tag{9}$$

where $K_5 = K_2/(K_1K_4^2)$. Equation 9 gives the relationship between the average undercooling ΔT, the temperature gradient G, and the fiber spacing λ, for an isothermal solidification front. As can be seen from (1) and (9), the relationship between temperature gradient G and undercooling ΔT is qualitatively the same as that between the growth rate V and undercooling. Applying the condition of growth at minimum undercooling ($(\partial\Delta T/\partial\lambda)_G = 0$) to eq 9 gives

$$\lambda^2 G = K_4 \tag{10a}$$

$$\frac{\Delta T}{\sqrt{G}} = \frac{2K_2}{K_4} \tag{10b}$$

$$\Delta T\lambda = 2K_2 \tag{10c}$$

The most important features of this qualitative analysis are that the temperature gradient influences interface undercooling in the same way as the growth rate and that the product of fiber spacing and undercooling is the same for both cases (case 1, growth with different V values at constant G; case 2, growth with different G values at constant V). Despite only qualitative character, these results are in good agreement with results obtained for lamellar eutectics,[11−14] and they indicate how and why the temperature gradient affects fiber spacing in directionally solidified eutectics with fibrous

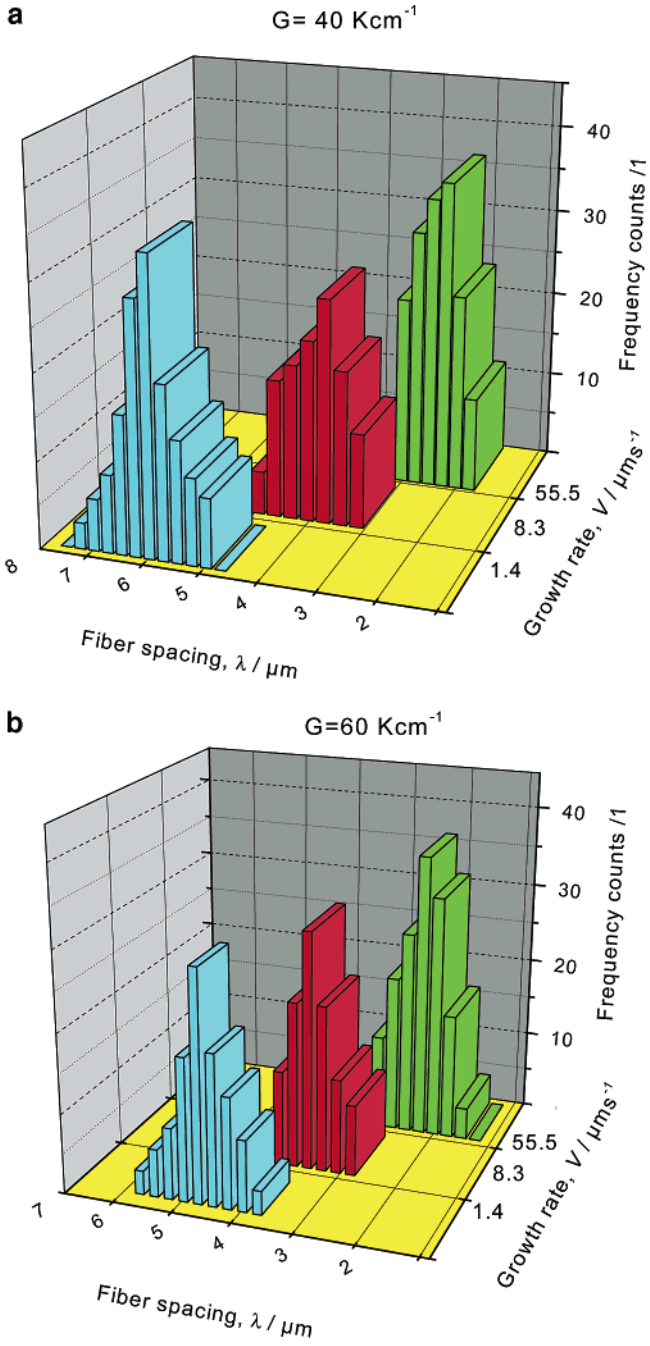

Figure 6. Histograms of the fiber spacing obtained at (a) 40 K cm^{-1} and (b) 60 K cm^{-1}.

morphology. Furthermore, they suggest that the temperature gradient also might be used to influence the final microstructure and consequently, the distance and diameter of nanowire arrays. However, further studies including more experimental results are required to confirm and quantify the observed effect.

(D) Spacing Selection. According to the Jackson and Hunt (J-H) theory,[3] the eutectic growth at constant growth rate occurs within a range of spacing values, near the extremum spacing which corresponds to the minimum undercooling. Fiber spacing smaller than the extremum spacing is unstable, while lamellar spacing larger than the extremum lamellar spacing is stable with respect to fluctuations in the solid/liquid interface. On the other hand, the maximum spacing

is limited by the motion of lamellar faults. Despite the J-H model predicting a wide range of spacings for steady-state growth at a certain growth velocity,[3] the experimental studies show that only a limited narrow range of eutectic spacing is actually selected by the system at a given growth velocity.[15−20] Although much effort has been made in the study of the spacing selection mechanism, the principle that controls the selection of spacing over this narrow band has not been established. Many investigations for eutectic spacing have been performed in the lamellar eutectics, whereas there is little concern for the relationship between the fiber spacing range and the controlling parameters in fibrous eutectic alloy. In addition, when one of the eutectic phases is faceted, as in the case of intermetallics that have high entropy of fusion, diffusion-controlled growth might be precluded and, hence, the solidification structure can result in irregular structure. Also, high entropy phases present difficulties in the branching phenomenon, which can lead to the interphase spacing selection problems.[19] Figure 6 presents the histograms of the fiber spacing for the employed growth conditions. These results clearly show that the fiber spacing distribution is independent of the growth condition, indicating that the NiAl−Re eutectic system does not show spacing selection difficulty, despite the presence of an intermetallic phase.

Conclusions. Thermodynamic aspects and growth control of Re nanowire arrays were investigated, and from the obtained results the following conclusions are drawn:

1. Uniform and well-aligned fibrous structures were obtained at low and intermediate growth rates of 1.4 and 8.3 μm s^{-1} and temperature gradients of 40 and 60 K cm^{-1}.

2. Fiber spacing and diameter increase with decreasing solidification rate according to power laws $\lambda^2 V = 2.21 \times 10^{-16}$ and $a^2 V = 2.65 \times 10^{-18}$ m^3 s^{-1}, respectively.

3. For the fixed growth rates, the fiber spacing and diameter were smaller at higher temperature gradients.

4. Qualitative thermodynamic analysis suggested that the temperature gradient influences interface undercooling in the same way as the growth rate, which correlates well with the phenomenon observed in lamellar eutectics.

5. Despite the presence of an intermetallic phase, fiber spacing selection problems were not observed.

Acknowledgment. The financial support of the Deutsche-Forschungs-Gemeinschaft through the project *Production of Nanowire Arrays through Directional Solidification and their Application* within the DFG Priority Program 1165 Nanowires and Nanotubes − From Controlled Synthesis to Function is gratefully acknowledged.

References

(1) Hassel, A. W.; Bello Rodriguez, B.; Milenkovic, S.; Schneider, A. *Electrochim. Acta* **2005**, *50*, 3033−3039.
(2) Hassel, A. W.; Bello Rodriguez, B.; Milenkovic, S.; Schneider, A. *Electrochim. Acta* **2005**, *51*, 795−801.
(3) Jackson, K. A.; Hunt, J. D. *Trans. Metall. Soc. AIME* **1966**, *236*, 1129−1140.
(4) Zenner, C. *Trans. AIME* **1946**, *167*, 550−558.
(5) Tiller, W. A. *Liquid Metals and Solidification*; ASM: Metals Park, OH, 1958.
(6) Kurz, W.; Sahm, E. *Gerichtet erstarrte eutektische Werkstoffe*; Springer: Berlin, 1975.
(7) Rablbauer, R.; Frommeyer, G., Stein, F. *Mater. Sci. Eng. A* **2003**, *343*, 301−307.
(8) Huang, X.; Zhang, Y.; Hu, Z. *Metall. Trans. JIM 38*, **1997**, *11*, 1016−1024.
(9) Kraft, R. W.; Albright, D. L. *Trans. Metall. Soc. AIME* **1961**, *22*, 195−203.
(10) Weart, H. W.; Mack, D. J. *Trans. Metall. Soc. AIME* **1958**, *212*, 664−670.
(11) Hogan, L. M.; Song, H. *Metall. Trans. A* **1987**, *18*, 707−716.
(12) Toloui, B.; Hellawel, A. *Acta Metall.* **1976**, *24*, 565−570.
(13) Elliott, R.; Glenister, S. M. D. *Acta Metall.* **1980**, *28*, 1489−1496.
(14) Çadirli, E.; Gündüz, M. *J. Mater. Process. Technol.* **2000**, *97*, 74.
(15) Trivedi, R.; Mason, J. T.; Verhoeven, J. D.; Kurz, W. *Metall. Trans. A* **1991**, *22*, 2523−2533.
(16) Seetharaman, V.; Trivedi, R. *Metall. Trans. A* **1988**, *19*, 1955−1964.
(17) Magnin, P.; Mason, J. T.; Trivedi, R. *Acta Metall. Mater.* **1991**, *19*, 469−480.
(18) Liu, J.; Elliott, R. *Acta Metall. Mater.* **1995**, *43*, 3301−3311.
(19) Ourdjini, A.; Liu, J.; Elliott, R. *Mater. Sci. Technol.* **1994**, *10*, 312−318.
(20) Aguiar, M. R.; Caram, R. *J. Cryst. Growth* **1996**, *166*, 398−402.

NL0514238